PCCP

Reaction mechanism of the astrochemical electron capture reaction $HCNH^+ + e^- \rightarrow HNC + H$: a direct *ab-initio* dynamics study

Hiroto Tachikawa*

Division of Molecular Chemistry, Graduate School of Engineering, Hokkaido University, Sapporo 060-8628, Japan. E-mail: hiroto@eng.hokudai.ac.jp; Fax: + 81 117067897

Received 19th July 1999, Accepted 13th September 1999

Electron capture processes of $HCNH^+$, $HCNH^+ + e^- \rightarrow HNC + H$, have been studied by means of direct *ab-initio* dynamics calculations in order to elucidate the reaction mechanism. The dynamics calculation of the $HCNH^+$ ion at 10 K showed that the structure of $HCNH^+$ is slightly deformed by thermal activation, while the bond angles in $HCNH^+$ are fluctuated around its equilibrium point. In the dynamics calculations of HCNH, we assumed that auto-ionization does not take place, once the $HCNH^+$ ion captures an electron. The dynamics calculations of HCNH following vertical electron capture of the $HCNH^+$ ion showed that two channels contribute to the reaction. One is a dissociation channel in which the hydrogen in the N–H bond is dissociated *via* a short-lived complex HCNH. The other channel is the complex formation in which a long-lived complex HCNH is formed after the electron capture. It was found that branching of the channels is dominated by the initial structure of $HCNH^+$ before the electron capture: the electron capture of $HCNH^+$ with larger bending angles leads to complex formation, whereas a trajectory from the structure close to the collinear skeleton leads to the direct dissociation channel. The reaction mechanism of the electron capture processes of $HCNH^+$ is discussed on the basis of these theoretical results.

1 Introduction

Electron capture processes by interstellar molecular ions such as $HCS^+ + e^-$ and $HCO^+ + e^-$ are important reactions in dark cold clouds[1–5] because the reactions proceed *via* the long-range Coulomb interaction.[1] As an astrochemical model, it has been considered that electron capture by the $HCNH^+$ ion (*i.e.* $HCNH^+ + e^-$) is the main reaction which forms HCN and HNC molecules in dark cold clouds. For the reaction pathway in $HCNH^+ + e^-$, two reaction channels

$$HCNH^+ + e^- \rightarrow HNC + H \qquad \text{channel 1}$$

$$\rightarrow HCN + H \qquad \text{channel 2}$$

are considered to be significant. In channel 1, the C–H bond is broken by the electron capture, whereas the hydrogen is dissociated from the N atom of $HCNH^+$ in channel 2. In both channels, the hydrogen dissociation takes place from the parent molecule HCNH. It has been considered that the main reaction pathway of $HCNH^+$ is channel 1. Both HNC and HCN molecules are known to be key molecules to synthesizing larger organic molecules in interstellar clouds,[1–5] so that the study of the origin of HCN/HNC is important in the field of current astrophysics.

The HNC/HCN abundance ratio varies in space from one source to another. In dark cold clouds[6] (*e.g.* TMC-1), the ratio of HNC/HCN is observed to be 1.55. In OMC-1, a region of high-mass star formation, the same abundance ratio changes drastically from 1/80 in the immediate vicinity of Orion-KL to values in the range of 1/5 for adjacent ridge positions.[7] These observations indicate that the ratio of HNC/HCN is dependent on temperature and that channel 1 is predominant at low temperatures below 10 K.

Recently, potential energy curves for the electron dissociative recombination process, $HCNH^+ + e^- \rightarrow HNC/HCN + H$, were calculated using large scale CI calculations.[8,17] It was shown that the lowest dissociative states of HCNH ($^2\Sigma^+$ symmetry) cross the ionic $HCNH^+$ state at its minimum geometry. The calculations support the astrophysical hypothesis of an equal formation of HCN and HNC in the $HCNH^+ + e^-$ dissociative recombination process. However, in these calculations, they assumed a high symmetry of $HCNH^+$/HCNH and only one dimensional potential energy curves were calculated for the reactions. Therefore, the dynamical features of the electron capture process are scarcely known because of a lack of dynamics studies.

In the present study, in order to elucidate the reaction mechanism of the electron capture processes of $HCNH^+$, direct *ab-initio* dynamics calculations using full dimensional potential energy surfaces are applied to the astrochemical dissociative recombination reaction of $HCNH^+$. In this paper, we focus our attention on channel 1, *i.e.* $HCNH^+ + e^- \rightarrow [HCNH]_{ver} \rightarrow HNC + H$, which has been considered as the main reaction channel of $HCNH^+$ in dark cold clouds (*e.g.* TMC-1), where $[HCNH]_{ver}$ means the HCNH molecule at the vertical electron capture point. It should be noted that the reaction of $HCNH^+$ with an electron has never been confirmed in the laboratory because of the chemical instability of $HCNH^+$ in the gas phase.

Dissociative recombination involves the capture of an electron by the positive ion to form the neutral molecule in an excited electronic state. If this state is repulsive, then dissociation takes place and the process is called direct. If this state is not repulsive, recombination may give a resonant state of an electronic state higher in energy than the ionization potential. The state can relax to lower energy states and the process is called indirect. In both cases, auto-ionization may take place. In this study, we assumed that the auto-ionization does not take place once the $HCNH^+$ ion captures an electron. Therefore, our model presented here is limited to the case of no auto-ionization or fast electronic energy relaxation. Also,

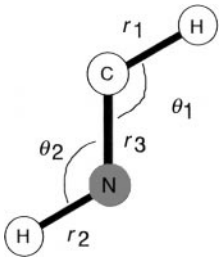

Fig. 1 Structures and geometrical parameters of the $HCNH^+$/HCNH system.

we did not consider the branching ratio of the channels, (*i.e*, channels 1, 2, and auto-ionization).

2 Computational methods

Usually, classical trajectory calculations are performed using an analytically fitted potential energy surface, as we have done previously.[9–11] However, it is not appropriate to predetermine the reaction surfaces of the present systems due to the large number of degrees of freedom ($3N - 6 = 6$ where N is number of atoms in the system). Therefore, in the present study, we applied the direct *ab-initio* dynamics method with all degrees of freedom. The details of the direct dynamics method is described elsewhere.[12–14] In the direct *ab-initio* dynamics calculation, we used a 6-311G(d,p) basis set for the electron capture process of $HCNH^+$ throughout. First, a trajectory calculation of the cation system $HCNH^+$ was carried out in order to obtain the initial structure of HCNH. The 6-311G(d,p) optimized geometry of $HCNH^+$ was chosen as an initial structure. At the start of the trajectory calculation, atomic velocities are adjusted to give a temperature of 10 K as the classical distribution. The temperature was defined by

$$T = \frac{1}{3Nk}\left\langle \sum_{i=1}^{N} m_i v_i^2 \right\rangle,$$

where N is number of atoms, v_i and m_i are velocity and mass of the i-th atom, and k is Boltzmann's constant. From the trajectory calculation of $HCNH^+$, we can determine the classical Franck–Condon (FC) region for the electron capture. Secondly, the initial geometries in the trajectory calculation of HCNH are sampled randomly from the geometrical configurations on the FC region generated in the trajectory calculation of $HCNH^+$. We calculated fifty trajectories for the HCNH system. The equations of motion for N atoms in a molecule are given by

$$\frac{dQ_i}{dt} = \frac{\partial H}{\partial P_j}$$

$$\frac{\partial P_j}{\partial t} = -\frac{\partial H}{\partial Q_j} = -\frac{\partial U}{\partial Q_j}$$

where $j = 1 - 3N$, H is the classical Hamiltonian, Q_j is Cartesian coordinate of the j-th mode and P_j is the conjugate momentum. These equations were numerically solved by the Runge–Kutta method. No symmetry restriction was applied to the calculation of the gradients in the Runge–Kutta method. The time step size was chosen as 0.10 fs, and a total of 10 000 steps were calculated for each trajectory. The drift of the total energy was confirmed to be less than 0.1% for an entire trajectory. It was also confirmed that the momentum of the center of mass and the angular momentum around the center of mass retained their initial values of zero. The program code of the direct *ab-initio* dynamics calculation was created by our group.

In order to obtain detailed structures and energetics of the $HCNH^+$ and HCNH complexes, *ab-initio* MO calculations were carried out at the HF and MP2 levels of theory with 3-21G and 6-311G(d,p) basis sets.[15] The coordinates used to describe the geometry of $HCNH/HCNH^+$ are schematically illustrated in Fig 1.

3 Results

A Structure of $HCNH^+$ at finite temperature

In order to obtain the structure of $HCNH^+$ at finite temperature, a trajectory for the $HCNH^+$ ion is calculated at constant temperature. We chose 10 K for a simulation temperature and 0.01 ps for a bath relaxation time. The optimized structure of $HCNH^+$ is chosen as the initial structure. A profile of the trajectory at 10 K is given in Fig. 2. The energy of the system calculated as a function of time was close to a constant value during the simulation (Fig. 2A). The three bond distances, r_1, r_2 and r_3, are plotted in Fig. 2B as a function of simulation time. The distances oscillate slowly around equilibrium points. The amplitude of r_1 is slightly larger than those of the other distances (r_2 and r_3). The angles (θ_1 and θ_2) oscillate slowly as clearly seen in Fig. 2C. These results indicate that the structure of $HCNH^+$ is fluctuated slowly around the equilibrium point even at low temperature and that it has a finite Franck–Condon (FC) region for electron capture, although the region is relatively narrow.

B Electron capture processes in $HCNH^+$

In order to describe the dynamics of HCNH, following the electron capture of $HCNH^+$, direct *ab-initio* dynamics calcu-

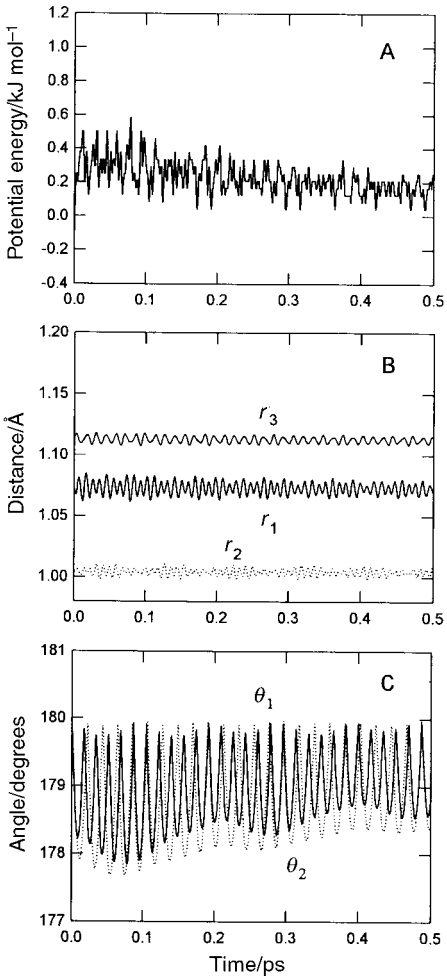

Fig. 2 A trajectory for the cation $HCNH^+$ plotted as a function of reaction time. The simulation is carried out at 10 K. (A) The potential energy of the reaction system, (B) interatomic distances r_1, r_2 and r_3 *vs.* time, and (C) angles θ_1 and θ_2 *vs.* time.

lations are carried out. The vertical electron capture of $HCNH^+$ is assumed. In addition, we assumed that autoionization does not take place once the $HCNH^+$ ion captures an electron. As suggested in the previous section, the structure of the H–C–N–H skeleton fluctuates around the collinear structure even at 10 K. The electron capture occurs from the FC region, so we chose several points on the FC region as the initial geometries in the dynamics calculations. A total of 50 trajectories are run from the selected points. From the dynamics calculations, it was found that two reaction channels are concerned as product channels. One is the dissociation channel in which the hydrogen in the C–H bond is dissociated from HCNH after the formation of a short-lived complex HCNH. The products in the dissociation channel are H + HNC. The other channel involves formation of a long-lived complex: the H dissociation does not take place and HCNH remains in the complex region.

Direct dissociation channel. A sample trajectory for the dissociation channel, leading to HNC + H product, is given in Fig. 3. Fig. 3A shows the potential energy as a function of reaction time, while the nuclear distances and bond angles are plotted as a function of time in Figs. 3B, C and D, respectively. It is seen that the reaction process is composed of three stages as shown in Fig. 3A. The first stage is the complex formation process (time = 0–0.06 ps): the neutral complex with a bent HCNH structure is formed immediately after the electron capture. However, the lifetime of the complex is very short (estimated to be *ca.* 0.05 ps). In the second stage, the trajectory passes over the reaction barrier (time = 0.06–0.07 ps). This process occurs very rapidly. The third stage is composed of the dissociation of the H atom from the parent molecule. The reaction is completed within a very short time (~0.2–0.3 ps), so that the reaction proceeds *via* the direct mechanism.

Here let us consider the dynamics in more detail. At the first stage, the bond angles (θ_1 and θ_2) are suddenly varied as a function of reaction time from *ca.* 180° to 80°, as shown in Fig. 3D. This structural change leads to the formation of an HCNH complex. However, in this complex formation, the excess energy of HCNH is not sufficiently distributed to the internal modes of the HCNH complex, so that the hydrogen is dissociated after the short-lived complex formation. This dissociation is clearly seen in Fig. 3B: the distance of r_1 increases linearly as a function of reaction time. Time dependence of the bond distances and angles of the fragment HNC (Figs. 3C and D) show that the internal modes of HNC are highly excited after the dissociation.

Snapshots for the sample trajectory are illustrated in Fig. 4. The trajectory corresponds to that given in Fig. 3. At time zero, the structure of HCNH is close to collinear. After very short time propagation (time = 0–0.02 ps), the H–C–N angle (θ_1) is largely bent as shown in Fig. 4 (time = 0.02 ps). The angle is close to 90°. At time 0.035 ps, the H–N–C angle (θ_2) is also bent. The structure of the HCNH is rapidly and largely deformed in the complex region. At 0.060–0.065 ps, the C–H bond is gradually elongated and then the hydrogen is dissociated from HNC. At 0.80 ps, it is seen that the hydrogen atom leaves the HNC molecule.

Complex formation channel. A sample trajectory for the complex formation channel, leading to the HCNH complex, is given in Fig. 5. Fig. 5A shows the potential energy of the system calculated as a function of reaction time, while the nuclear distances and bond angles are plotted as a function of time in Figs. 5B and C, respectively. After electron capture by $HCNH^+$, the potential energy of the system (PE) decreases suddenly as a function of time up to -190 kJ mol^{-1}. The energy change is caused by a rapid deformation of the HCNH

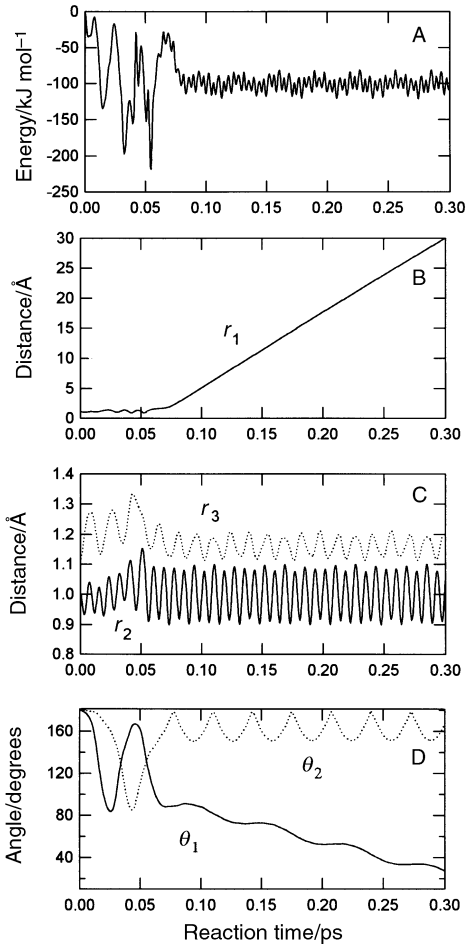

Fig. 3 A sample trajectory for the dissociation channel of HCNH formed by the vertical electron capture of $HCNH^+$ from the equilibrium point. (A) The potential energy of the reaction system, (B) interatomic distance, r_1, (C) intramolecular distances r_2 and r_3, and (D) angles θ_1 and θ_2 *vs.* time. Snapshots of the structures for the trajectory are given in Fig. 4.

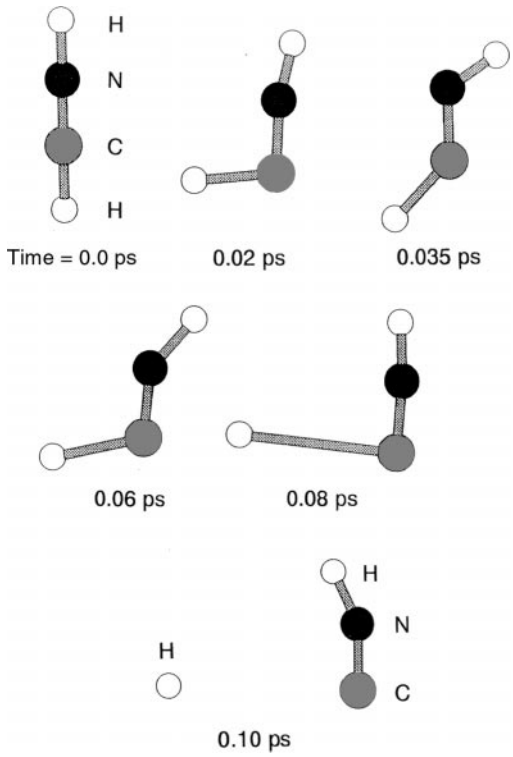

Fig. 4 Snapshots of HCNH following the vertical electron capture of $HCNH^+$.

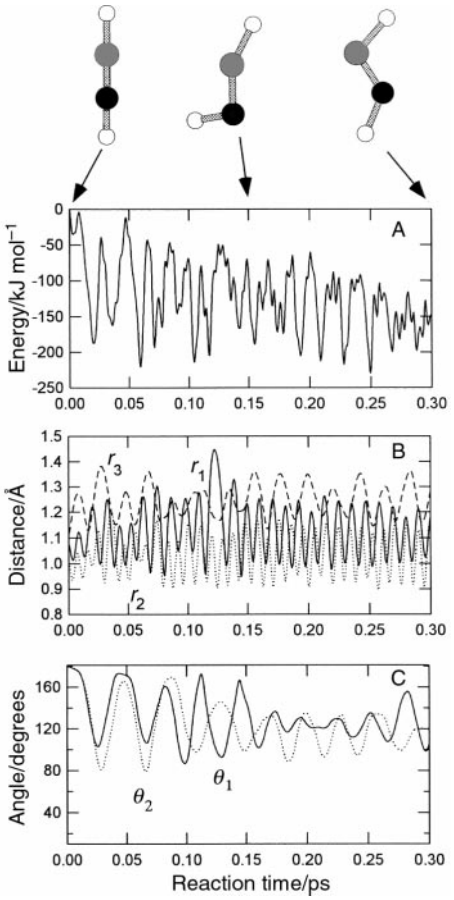

Fig. 5 A sample trajectory for the complex formation channel of HCNH formed by the vertical electron capture by $HCNH^+$ from a non-equilibrium point. (A) The potential energy of the reaction system, (B) interatomic distances r_1, r_2 and r_3, and (C) angles θ_1 and θ_2 *vs.* time. Snapshots of the structures for the trajectory are illustrated in the upper panel.

skeleton: the bending angles (θ_1 and θ_2) are varied simultaneously to each other as shown in Fig. 5C. The HCNH complex is directly formed by the electron capture. This feature is very different from that of the dissociation channel (*i.e*, the angle θ_1 is more rapidly changed than that of θ_2 as shown in Fig. 3D). In the complex region, all bonds and angles are strongly vibrated because the excess energy is efficiently transferred into the internal modes of HNCH. For this trajectory, the complex was not decomposed to H + HCN or H + HNC within 2 ps, meaning that this channel leads to a long-lived complex formation. Snapshots for the sample trajectory are illustrated in Fig. 5 (upper illustration). At time zero, the structure of HCNH is close to collinear, but the angles θ_1 and θ_2 are slightly smaller than 180°. After a very short time propagation (time = 0–0.02 ps), the angle is largely bent and the complex is directly formed after electron capture. The structure of HCNH is rapidly and largely deformed in the complex region.

Summary of the dynamics calculations. Similar calculations were carried out for a total of 50 trajectories. The calculations gave the products from the two reaction channels 1 and 3

$$HCNH^+ + e^- \rightarrow HNC + H \qquad \text{channel 1}$$

$$\rightarrow HCNH \qquad \text{complex formation, channel 3}$$

while the main channel is the complex formation. For all trajectories in the dissociation channel (*i.e.* channel 1, and the products HNC + H), it was found that the trajectories pass *via* the short-lived complex, although the life-time of the complex is negligibly small. The relative translational energy between fragments (*i.e.* H and HNC) is distributed from 42 to 63 kJ mol^{-1}. The average of the relative translational energies is calculated to be 50.2 kJ mol^{-1} which corresponds to 40% of the total available energy. In the complex formation channel, the complex has a large internal energy, and the bond distances and angles of HCNH are highly excited in the potential well.

C Structure of the HCNH complex

The dynamics calculations showed that a long-lived complex is formed in the complex formation channel after electron capture by $HCNH^+$. In this section, the detailed structure of the HCNH complex is calculated by means of the *ab-initio* MO calculations. The geometry of the HCNH neutral complex is fully optimized by means of the HF/6-311G(d,p) and MP4SDQ/6-311G(d,p) calculations. The optimized geometrical parameters are summarized in Table 1. All calculations gave similar results. It was found that the HCNH molecule is strongly bent, which is much different from the feature of $HCNH^+$ (*i.e.* collinear). From the most sophisticated calculation (MP4SDQ/6-311++G(d,p) level), it is expected that the rotational constants of HCNH are 420.83, 39.26 and 35.91 GHz.

The energy calculations at the MP4SDQ/6-311G(d,p) level indicate that the HCNH complex is more stable in energy than its dissociation limits (HNC + H and HCN + H). The stabilization energies of HCNH measured from (HNC + H) and (HCN + H) are calculated to be 1.36 and 0.71 eV, respectively. These results strongly indicate that the existence of the HCNH complex in dark cold clouds is possible.

The potential energy curves for channel 1 are calculated at both the MP4SDQ/6-311G(d,p) and HF/6-311G(d,p) levels as a function of C–H distance (r_1) in order to validate the HF/6-311G(d,p) calculation. The shapes of the potential curves are similar to each other. This means that the HF/6-311G(d,p) calculation may be enough to simulate qualitatively the reaction dynamics of HCNH.

4 Discussion

In this study, direct *ab-initio* dynamics calculations have been applied to the reaction dynamics of the astrochemical electron

Table 1 Optimized structures calculated at several levels of theory[a]

	$HCNH^+$ [b]		HCNH[c]		
	HE/6-311G(d,p)	MP4SDQ/6-311G(d,p)	HE/6-311G(d,p)	MP4SDQ/6-311G(d,p)	MP4SDQ/6-311++G(d,p)
r_1	1.0722	1.0822	1.0831	1.1004	1.0994
r_2	1.0041	1.9164	1.0075	1.0185	1.0186
r_3	1.1132	1.1414	1.2288	1.2208	1.2214
θ_1			127.4	124.9	125.6
θ_2			114.3	118.87	119.4

[a] Bond length and angles are in Å and degrees, respectively. [b] Collinear structure is assumed. [c] C_s structure is assumed.

capture process, $HCNH^+ + e^-$, in order to elucidate its reaction mechanism. The dynamics calculation of the $HCNH^+$ ion at 10 K showed that the structure of $HCNH^+$ is deformed by thermal activation and the bond angles of $HCNH^+$ are slightly vibrated around the collinear. The dynamics calculation of HCNH, following vertical electron capture by the $HCNH^+$ ion, showed that the hydrogen is dissociated directly from the HCNH molecule *via* a short-lived complex HCNH, although the lifetime of the complex is negligibly small. The reaction proceeds *via* a direct mechanism. As a product from the other channel, a long-lived complex HCNH is found. The analysis of initial conditions of HCNH indicates that HCNH with larger bending angles leads to the complex formation, whereas a trajectory from the structure close to the collinear skeleton leads to the dissociation channel *via* a direct mechanism. From these results, it is expected that the HCNH complex exists as well as the dissociated molecules (HNC and HCN) in dark clouds if HNC and HCN are formed by the electron capture by $HCNH^+$. The branching ratio of channels 1 and 3 is roughly estimated to be 1/5, meaning that a large amount of the complex exists in dark clouds. We did not find channel 2 (the products are HCN + H) because we considered only dynamics in the case of non-excess energy of HCNH at the initial point of the trajectory calculation. If HCNH has excess energy, channel 2 may be open.

The Reaction model

As a summary of this work, we would like to propose a model for channel 1. Fig. 6 shows potential energy curves (PECs) along the reaction coordinate for channel 1. Upper and lower curves indicate the PECs of $HCNH^+$ and HCNH, respectively. If the vertical electron capture takes place from the collinear HCNH skeleton, HCNH is directly dissociated into the product (HCN + H) without complex formation. In this case, the trajectory proceeds along the dashed curve. On the other hand, capture from a slightly bent form of $HCNH^+$ leads to formation of a short-lived complex and then H-dissociation takes place immediately. This is indirect dissociation. In this case, the trajectory proceeds along the solid curve. The dashed arrows indicate the structural relaxation of HCNH. Electron capture from larger bending angles of $HCNH^+$ leads to the formation of the long-lived complex. The trajectory remains in the HCNH complex region. These results indicate that the formation of HCN and HNC is strongly affected by the temperature of interstellar clouds. Actually, these feature are observed by recent astronomical measurements.[18]

Mechanism of the HNC and HCN formation in interstellar clouds

It has been observed that the branching ratio (HNC/HCN) is significantly varied as a function of temperature. In dark clouds (*e.g.* TMC-1, temperature of about 10 K), the ratio is 1.55. In Orion-KL (higher temperatures), the ratio HNC/HCN is observed to be 1/5, whereas it is changed to 1/80 in a region of high-mass star formation (significantly higher temperatures, *e.g.* OMC-1). In this section, we will discuss the formation mechanism of HNC and HCN in interstellar clouds.

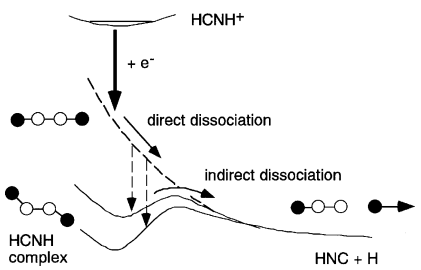

Fig. 6 Reaction model for the dissociative electron capture by $HCNH^+$.

The present calculations show that at very low temperature (below 10 K which is close to the temperature in dark clouds) the electron capture by $HCNH^+$ leads to the HNC + H product *via* direct mechanism because $HCNH^+$ has a near-linear structure at 10 K. In addition to the product (HNC + H), the complex HCNH is also formed as the other major channel by electron capture. As a minor channel, the HCN + H product is formed if the excess energy is transferred efficiently to HCNH at the initial point.

At intermediate temperatures which are close to that in the spherical region of Orion-KL, $HCNH^+$ is vibrated and the bending angles are varied as a function of time. The population of the collinear form of $HCNH^+$ is less than that at the low-temperature (10 K). Therefore, contribution to the complex formation becomes larger than that of 10 K. The complex HCNH formed by the electron capture may be decomposed thermally into HCN + H because the activation barrier for HCN + H channel is about 1 kJ mol^{-1} lower in energy than that for HNC + H channel (at the MP4SDQ/6-311G(d,p) level). At high-temperature regions (*e.g.*, a region of high-mass star formation), $HCNH^+$ is strongly vibrated, so that almost all products may be the HCNH complex. The complex is decomposed easily into HCN + H due to high temperature. The ratio of HCN is significantly larger than that of HNC. Thus, the present model may reasonably explain the observation in dark clouds.

Concluding remarks

We have introduced several approximations in calculating the potential energy surface and in treating the reaction dynamics. Firstly, we assumed that HCNH has two electronic states ($1^2\pi$ and $1^2\Sigma$) and no excess energy at the initial step of the trajectory calculation (time = 0.0 ps). In addition, the momentum vectors (velocities) of atoms were assumed to be zero because of the very low temperature (10 K). These assumptions may cause a slight change of lifetime of the HCNH complex and energy distribution of dissociating products. In the case of higher excess energy, the dissociation into HNC and H may occur more efficiently. Moreover, channel 2 is open as a product channel. This effect was not considered in the present calculations. It should be noted therefore that the present model is limited to the case of no excess energy.

Secondly, in the dynamics calculations of HCNH, we assumed that auto-ionization does not take place, once the $HCNH^+$ ion captures an electron. If auto-ionization occurs efficiently with electron capture, the reaction channels would be affected. Therefore, the present model is limited to the case of no auto-ionization. A more accurate calculation is probably necessary for obtaining reliable qualitative features. Also, it was assumed that the reaction proceeds on the PES for the ground state of HCNH. As a preliminary calculation, we considered quartet state PES for dynamics calculation of HCNH. It was found that the new reaction channel

$$HCNH^+ + e \rightarrow {}^4(HCNH) \rightarrow HC + HN$$

is open.[16] The meta-stable complex on the quartet state PES, ^{4}(HCNH), is directly dissociated into HC and HN radicals. The C–N bond-breaking occurs without complex formation. Despite the several assumptions introduced here, the results enable us to obtain valuable information on the mechanism of the electron capture process by $HCNH^+$.

Acknowledgements

The author is indebted to the Computer Center at the Institute for Molecular Science (IMS) for the use of the computing facilities. The author acknowledges partial support from a

Grant-in-Aid from the Ministry of Education, Science, Sports and Culture of Japan.

References

1 E. Herbst, *Angew. Chem., Int. Ed. Engl.*, 1990, **29**, 595.
2 W. T. Huntress, Jr. and G. F. Mitchell, *Astrophys. J*, 1979, **231**, 456.
3 D. Smith, *Chem. Rev.*, 1992, **92**, 1473.
4 G. Bertheier, S. Chekir, N. Jaidane, F. Pauzat, Y. Tao and P. Vermeulin, *J. Mol. Struct.*, 1983, **94**, 327.
5 H. Suzuki, *Astrophys. J.*, 1983, **272**, 579.
6 W. M. Irvine and F. P. Schloerb, *Astrophys. J.*, 1984, **282**, 516.
7 P. Schilke, M. C. Walmsley, G. Pineau des Forets, E. Roueff, D. R. Flower and S. Guilloteau, *Astron. Astrophys.*, 1992, **256**, 595.
8 D. Talbi and Y. Ellinger, *Chem. Phys. Lett.*, 1998, **288**, 155.
9 (*a*) M. Karplus, R. N. Porter and R. D. Sharma, *J. Chem. Phys.*, 1965, **43**, 3259; (*b*) M. Baer, *The Theory of Chemical Reaction Dynamics*, ed. M. Baer, Chemical Rubber, Boca Raton, 1985, vol. 2, ch. 4.
10 H. Tachikawa, *Trends Phys. Chem.*, 1997, **6**, 279.
11 (*a*) H. Tachikawa, *J. Chem. Phys.*, 1998, **108**, 3966; (*b*) H. Tachikawa, K. Ohnishi, S. Hamabayashi and H. Yoshida, *J. Phys. Chem. A*, 1997, **101**, 2229; (*c*) H. Tachikawa, *J. Phys. Chem.*, 1995, **99**, 225.
12 H. Tachikawa, *J. Phys. Chem. A*, 1998, **102**, 7065.
13 H. Tachikawa and M. Igarashi, *J. Phys. Chem. A*, 1998, **102**, 8648.
14 H. Tachikawa, *J. Phys. Chem. A*, 1997, **101**, 7475.
15 *Ab-initio* MO calculation program, Gaussian 94, Revision E.2, M. J. Frisch, G. W. Trucks, H. B. Schlegel, P. M. W. Gill, B. G. Johnson, M. A. Robb, J. R. Cheeseman, T. Keith, G. A. Petersson, J. A. Montgomery, K. Raghavachari, M. A. Al-Laham, V. G. Zakrzewski, J. V. Ortiz, J. B. Foresman, J. Cioslowski, B. B. Stefanov, A. Nanayakkara, M. Challacombe, C. Y. Peng, P. Y. Ayala, W. Chen, M. W. Wong, J. L. Andres, E. S. Replogle, R. Gomperts, R. L. Martin, D. J. Fox, J. S. Binkley, D. J. Defrees, J. Baker, J. P. Stewart, M. Head-Gordon, C. Gonzalez, and J. A. Pople, Gaussian, Inc., Pittsburgh PA, 1995.
16 H. Tachikawa, unpublished data.
17 Y. Shiba, T. Hirano, U. Nagashima and K. Ishii, *J. Chem. Phys.*, 1998, **108**, 698.
18 T. Hirota, S. Yamamoto, H. Mikami and M. Ohishi, *Astrophys. J.*, 1998, **503**, 717.

Paper 9/05817F